Hydroxyl Radical Reactions with Phenol as a Model for Generation of Biologically Reactive Tyrosyl Radicals

Maria J. Lundqvist[†,‡] and Leif A. Eriksson*[,†]

Department of Quantum Chemistry, Box 518, Uppsala University, 751 20 Uppsala, Sweden, and Department of Chemical Engineering, Box 325, Mälardalen University, 631 05 Eskilstuna, Sweden

Received: August 24, 1999; In Final Form: November 12, 1999

Reactions of the hydroxyl radical with phenol, as model for the generation of biologically harmful tyrosyl radicals, have been investigated using high level quantum chemical techniques. Hybrid Hartree−Fock density functional theory (HF-DFT) calculations, using the B3LYP functional, and standard ab initio HF and second-order Moller−Plesset perturbation theory (MP2) calculations are employed to locate addition complexes, transition state structures, and products for OH addition to the various positions in the aromatic ring, as well as for direct abstraction of the phenolic hydrogen and for the observed water elimination from 1,2-dihydroxy-cyclohexadienyl. Although the different methods yield some variation in terms of barrier heights and addition complex geometries, a consistent picture is provided by the DFT and spin projected MP2 data. In summary the present calculations support previous experimental observations reporting essentially diffusion-controlled mechanisms for ring OH addition and direct hydrogen abstraction, but a significantly slower rate for water elimination of 1,2-dihydroxy-cyclohexadienyl. The computed energy surfaces are analyzed in relation to explicit product mixtures and reaction rates previously reported experimentally for OH radical additions to tyrosine and to phenol.

Introduction

Hydroxyl radicals play an important role in creating unwanted radical centers or chemical modifications in biological media. OH radicals may be generated by degradation of peroxides or free radicals, or result from radiolytic cleavage of water, and have been shown to be one of the main sources of secondary radicals through either hydrogen atom abstraction or hydroxyl radical addition reactions. The secondary radical centers can be either amino acids, DNA components, cofactors or phospholipids, and are in turn often the source of rapid chain reaction sequences, e.g., leading to covalent protein−protein or DNA−protein linkage, DNA strand breakage, and more.[1,2] In the present study we have focused on a detailed investigation of the actual reaction mechanisms leading to product formation and subsequent reaction sequences between hydroxyl radicals and a model of the aromatic amino acid tyrosine. The net reactions involve the removal of the phenolic hydrogen to generate tyrosyl radicals, a known source for DNA−protein cross-links when exposing nucleohistones to high energy radiation[3]:

$$\mathrm{Tyr{-}OH} + {}^{*}\mathrm{OH} \rightarrow \mathrm{Tyr{-}O^{*}} + \mathrm{H_2O} \qquad (1)$$

$$\mathrm{Tyr{-}O^{*}} + \mathrm{base} \rightarrow \mathrm{Tyr{-}O{-}base^{*}} \qquad (2)$$

where "base" denotes one of the DNA bases (most commonly thymine). Evidence also exists for the formation of *o*-*o*′-dityrosine cross-links in lipoproteins, upon exposure to OH radicals.[4]

Tyrosyl radicals are also employed by nature for radical transport reactions in, e.g., ribonucleotide redcutase and in photosystem II,[5] and have been carefully characterized using electron spin resonance (ESR) and electron−nuclear double resonance (ENDOR) techniques[6] as well as with accurate theoretical methods.[7] It is well established that the preferred radical form of tyrosine is neutral and uses the phenolic oxygen radical center as hydrogen atom (or electron + proton) mediator.

The product mixtures and reaction rates between tyrosine and radiolytically generated OH radicals have been investigated in neutral, N_2O-saturated aqueous solution by Solar et al. using a combination of pulse radiolysis and time-resolved absorption spectroscopy techniques.[8] A summary of the main results is displayed in Figure 1. As expected, the OH radical addition reactions are very fast − close to diffusion controlled. Noteworthy is the high preference for *o*-hydroxy products (50% of the product mixture) and the relatively slow reaction rate for water elimination; on the order of 10^5 times slower than the addition reactions. We also note that the rate of direct elimination of the phenolic hydrogen is claimed to be ca. 10 times slower than for OH radical addition to the ring. The reported data largely agree with earlier total rate constants obtained under acidic conditions.[9]

In addition, Raghavan and Steenken have reported an estimate of the product yields for OH radical additions to the various ring positions in phenol,[10] given in parentheses in Figure 1, based on similar techniques. There is an apparent strong effect of the para substituent on the relative product yield. In the presence of the alanine substituent at C1 of tyrosine (i.e., the peptide backbone), steric hindrance indicates that large quantities of the OH radicals are steered over to the meta position despite the lesser spin density compared to para.

The present study is part of a larger effort in understanding the fundamental aspects of radicals in biology. Using the same methodology as in the present work, we have previously investigated the OH radical addition reactions to imidazole (the

* Corresponding author: leif.eriksson@kvac.uu.se.
† Uppsala University.
‡ Mälardalen University.

10.1021/jp993011r CCC: $19.00
Published on Web 01/05/2000

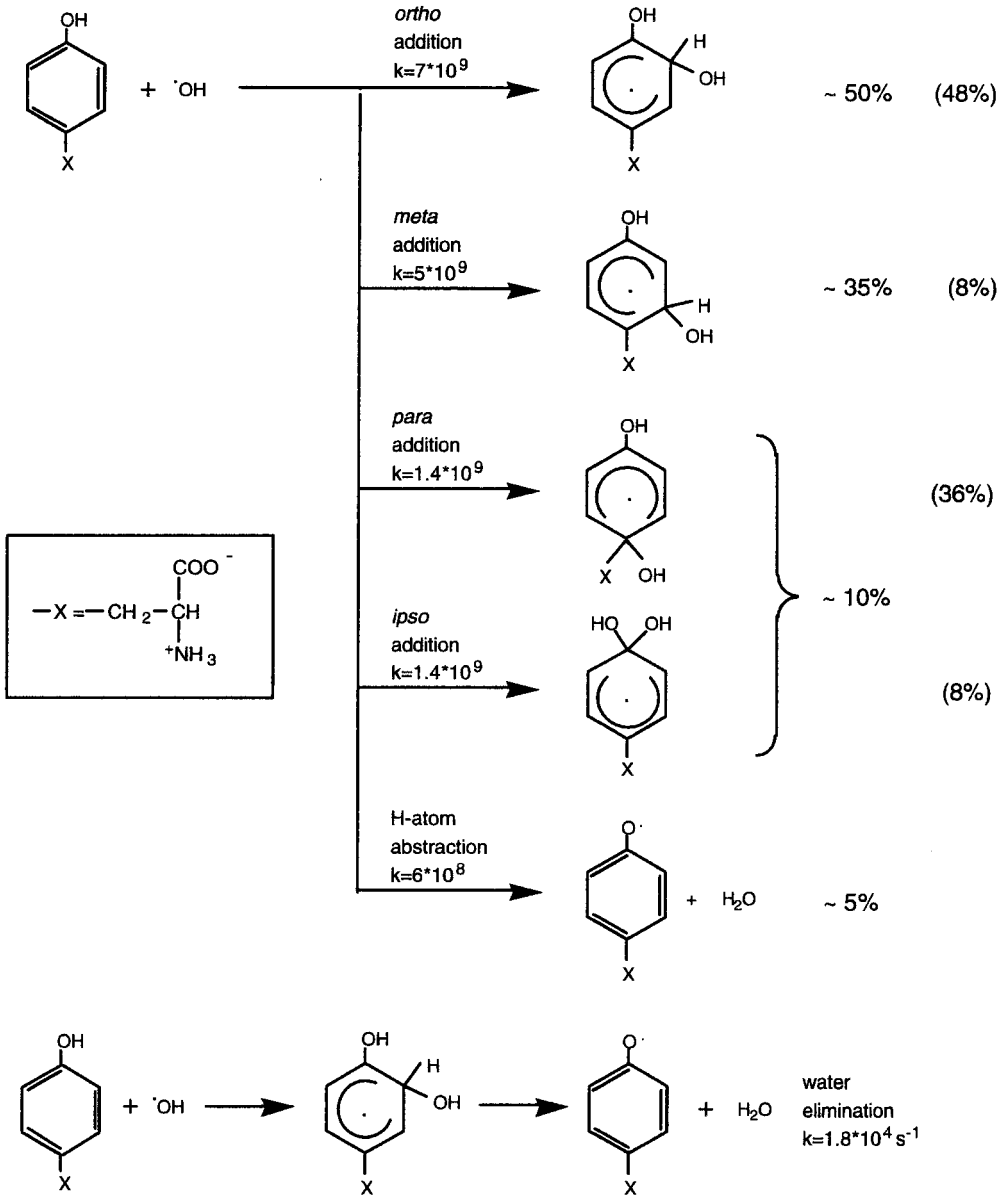

Figure 1. Summary of reaction rates and product mixture from reaction of tyrosine with radiolytically generated hydroxyl radicals. From Solar et al.[8] Rates in $dm^3\ mol^{-1}\ s^{-1}$ unless otherwise indicated. Product yields given in parentheses are from reactions between phenol and OH radicals, as reported by Raghavan and Steenken.[10]

ring system of amino acid histidine)[11] and the five DNA/RNA bases.[12] The individual spectroscopic (ESR) parameters of tyrosyl[7] and hydroxyl[13] radicals, as well as effects of ring substitutent modifications observed in various proteins on the phenolic OH bond strength[14] and spectroscopic properties[15,16] of tyrosine, have also been explored.

Theoretical Method

In the present work, only reactions between OH radicals and phenol were investigated, including OH radical additions to the phenol ring, direct H-atom abstraction, and water elimination reactions. Water elimination assisted by an additional water molecule was also considered. For easy comparison with tyrosine, we employ the same numbering scheme for the ring atoms; i.e., the carbon bonded to the phenolic oxygen is denoted C4, whereas C1 is used for the carbon in para position.

Optimization and frequency calculations were carried out at the HF, MP2,[17] and B3LYP[18] levels of theory, using a double-ζ basis set augmented by polarization functions on all atoms (6-31G(d,p)).[19] These were followed by single-point energy calculations using the larger 6-311G(2df,p) basis set,[19] and to which the zero-point vibrational energy effects (ZPE) from the lower level frequency calculations were added. For several of the transition states, IRC calculations were performed to ensure that the correct reactants and products were associated therewith. In addition, all stable points on the HF/6-31G(d,p) energy surfaces were also characterized by MP2 and B3LYP calculations employing the larger basis sets. The energetics are referred to as X//Y, meaning X/6-311G(2df,p) single-point calculations on Y/6-31G(d,p) optimized structures (plus Y/6-31G(d,p) ZPE corrections). Previous work has shown that the B3LYP level of theory tends to underestimate reaction barriers for OH radical addition,[10−12] whereas MP2 calculations have been used with great success in the past to study hydroxyl radical addition and abstraction reactions.[20−25] In addition, some work has shown that HF optimizations followed by single-point MP2 calculations render similar barriers as when optimizing the full structure at the MP2 level.[21] In other cases, however, correlation has proven

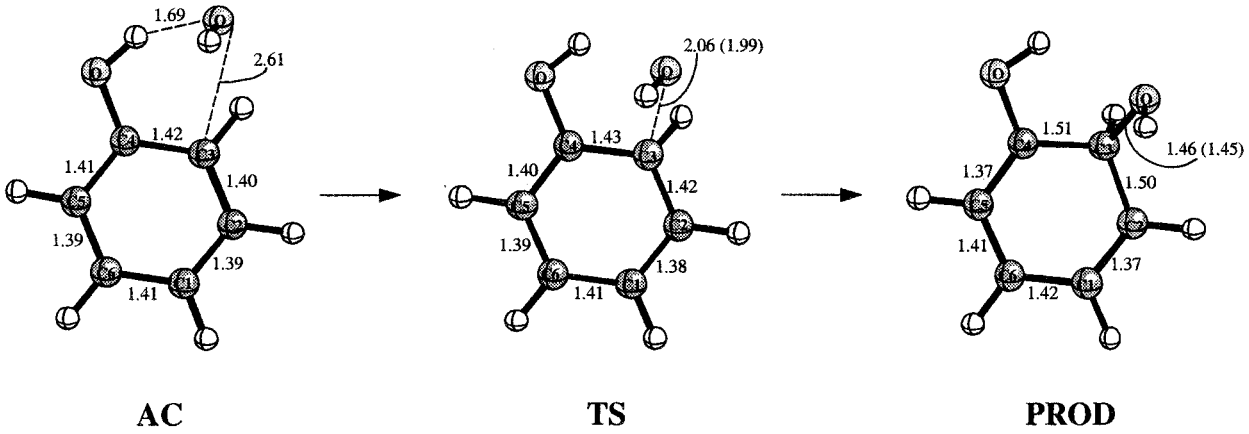

Figure 2. Optimized structures for addition complex, transition state, and product of hydroxyl radical addition to the ortho position of phenol. Relevant structural parameters from the B3LYP/6-31G(d,p) and (in parentheses) MP2/6-31G(d,p) calculations are included.

vital for accurate transition state structures, and even more so for the barrier heights.[20−22] Of relevance to the present study is, e.g., also the work of Skokov and Wheeler showing B3LYP to give barriers for H-atom abstraction by OH from H_2 and from CH_4 of ca. 4 kcal/mol, in close agreement with experimental data, after corrections for BSSE and ZPE, thermal corrections, and estimates of tunneling.[26]

For all DFT calculations spin contamination was (as expected) negligible; $\langle S^2 \rangle < 0.79$ for all stationary points. At the HF and MP2 levels, on the other hand, $\langle S^2 \rangle$ values were typically in the range 0.95−1.35, and we will thus only employ spin projected data for the final analysis. Isotropic hyperfine coupling constants (HFCC) were evaluated in the larger basis set calculations, using the standard forumla based on unpaired spin density distributions ("Fermi contact terms").[27] All calculations were performed using the *Gaussian 94*[28] and *Gaussian 98*[29] program suites.

Results

A. OH Addition to Ring. In Figure 2 we display the optimized addition complex (AC), transition state (TS), and product for OH addition to the ortho position in phenol, computed at the B3LYP/6-31G(d,p) level. IRC calculations and extensive potential energy searches revealed that the ipso and ortho additions share a common addition complex structure, as do the meta and para adducts, at both B3LYP and HF levels of theory. Somewhat surprisingly, no addition complexes could be determined at the MP2/6-31G(d,p) level despite significant efforts. The optimized geometries obtained with the different methods are highly similar for all of the various stationary points, generally within 0.04 Å for all bonds in the same molecule. The main difference occurs for the distance from the OH oxygen to the ring in that the HF ACs display much longer distances between the OH group and the ring: 2.11 Å between the phenolic hydrogen and the adding oxygen in case of the ortho/ipso AC, to be compared with 1.69 Å at the B3LYP level, and 3.75 Å at the HF level between the adding O and C1 in the case of the meta/para AC, to be compared with 2.39 Å at the B3LYP level. The very large distances in the HF ACs, coupled with the high degree of spin contamination, may be one rationale for the difficulty in locating stable addition complexes at the MP2 level.

For the TSs, the HF optimized $HO\cdots C_{ring}$ distances are instead the shortest (ca. 1.9 Å), whereas the corresponding MP2 (B3LYP) distances are 1.95−1.99 (2.02−2.06) Å. In the ortho, meta, and para transition structures the OH group is oriented such that the hydrogen points toward the interior of the ring. In case of the ipso TSs, the phenolic hydrogen rotates out of the ring plane to form a hydrogen bond to the adding oxygen. Already in the TSs do we see a slight elongation of the two C−C bonds in the ring, connecting to the addition center (B3LYP/6-31G(d,p): 1.42−1.43 vs 1.38−1.41 Å for the remaining bonds). The effect is more pronounced at the HF level, and less so at the MP2 level of theory. In the products, finally, the C−C bonds connecting to the addition center are 1.50−1.51 Å at all levels, and the two subsequent C−C bonds away from the addition center (e.g., C2−C3 and C5−C6 for the ipso and para adducts) have a more pronounced double bond character. The orientation of the added hydrogen observed for the TSs is maintained for the products.

Energetically, the common meta/para addition complex is the least stable of the two, lying 2−5 kcal/mol below the isolated reactants. The other AC (ipso/ortho) is between 1 and 4 kcal/mol more stable, depending on theoretical method, with the most pronounced difference observed at the B3LYP//B3LYP and B3LYP//HF levels. The large spin contamination at the HF and MP2 levels, as mentioned above, is clearly reflected in the barrier heights. Using the geometries obtained at the HF/6-31G-(d,p) level, the spin unprojected barrier heights are 29 ± 2 kcal/mol at the MP2/6-311G(2df,p) level (ca. 15 kcal/mol at the HF/6-311G(2df,p) level); after spin projection the barriers drop by as much as 27−28 kcal/mol to between 1 and 3.5 kcal/mol at the MP2 level and −13 kcal/mol at the HF level!

The barriers obtained at the B3LYP//B3LYP level are very similar to those obtained at the PMP2//HF level, 1−6 kcal/mol. If we instead use the HF optimized structures, we note negative barriers (1−2 kcal/mol) for the ortho and para transition structures and zero barrier for the meta form at the single point B3LYP level. Based on energetics obtained for OH radical addition to other aromatic ring systems, such as imidazole and the various DNA/RNA bases,[11,12] and the very high reaction rates reported by Solar et al.,[8] the most trustworthy results appear to be the B3LYP//B3LYP and PMP2//HF data. In Figure 3 we display these two sets of energetics for the different ring addition positions.

According to these sets of data, the most stable (dominant) addition complexes are the ipso/ortho ones. The lowest transition barriers are observed for the ortho and para forms (0.8−1.8 and 0.9−1.5 kcal/mol, respectively), followed by the barrier for the meta adduct (2.0 vs 2.6 kcal). The data are consistent with the highest product yeild for the ortho OH adduct seen experimentally[8,10] in that we will have two possible addition sites there compared with the para position. For phenol, there should hence

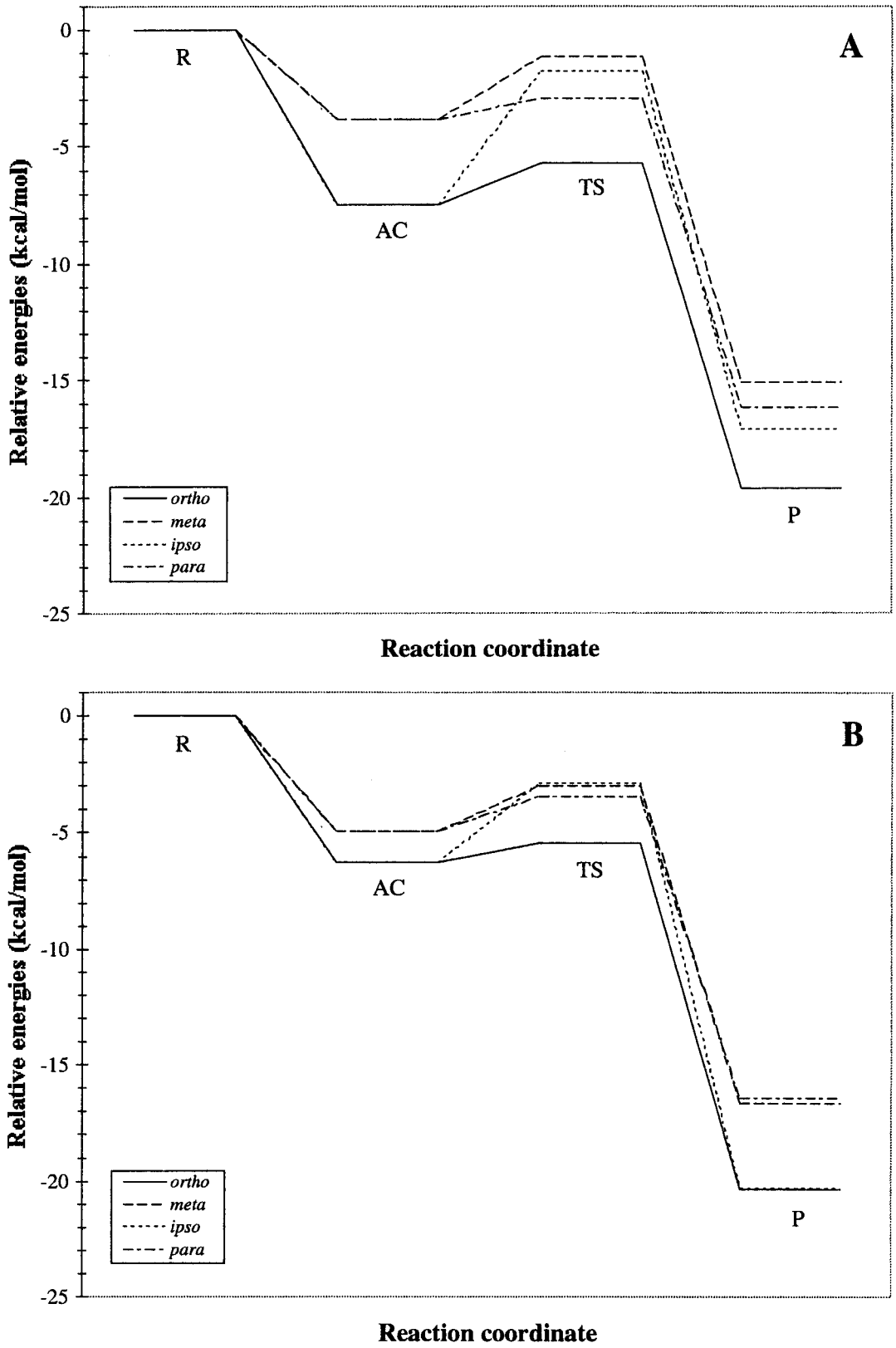

Figure 3. Energy surfaces for OH radical addition to the different ring sites, obtained from (A) ZPE corrected B3LYP/6-311G(2df,p) calculations on B3LYP/6-31G(d,p) optimized structures, and (B) the corresponding PMP2/6-311G(2df,p)//HF/6-31G(d,p) calculations.

be a slight preference for the *o*-OH adduct,[10] whereas in the full amino acid tyrosine it is reasonable to assume that addition to this site will be somewhat crowded and hence have a reduced reaction rate.[8] The largest barrier is found for the ipso form: 3.4−5.7 kcal/mol, explaining the lowest product formation for this species.

The products, finally, lie 14−21 kcal/mol below the isolated reactants. The thermodynamically most favored product is the ortho form, followed by ispo, para, and, of highest relative energy, the meta OH adduct of phenol. At the PMP2//HF level, the meta and para products are essentially degenerate in energy. It should be noted that all points on the energy surfaces lie below

TABLE 1: ^{1}H and ^{17}O Isotropic Hyperfine Coupling Constants (gauss) for the Different OH Addition Products to Phenol, Computed at the B3LYP/6-311G(2df,p)//B3LYP/6-31G(d,p) Level (C1 is assumed connecting to the amino acid backbone; phenolic oxygen binds to C4)

atom	ortho	meta	para	ipso
H2	−8.2	37.3	−9.4	3.9
H3	40.0	−7.6	3.2	−9.6
H5	3.3	−12.4	3.2	−9.6
H6	−11.7	3.5	−8.6	3.9
O4	−2.7	1.2	−4.1	−13.0
H(O4)	−0.9	0.0	−2.6	1.2
O_{add}	−14.0	−12.8	−15.3	−13.0
$H(O_{add})$	−1.0	−1.3	−1.8	1.2

the isolated reactants (except in the case of the spin unprojected calculations where the barriers are severely endothermic) and that the reactions will hence proceed to the desired product once the reactants are sufficiently close.

The energy surfaces were also evaluated using the smaller 6-31G(d,p) basis set, with and without ZPE effects. Relative to the isolated reactants, the larger basis set leads throughout to less stable compounds, by 0.2−0.8 kcal/mol. Adding the zero-point vibrational energies also leads to decreased stability by raising the energies of the ACs and TSs ca. 1.7 kcal/mol and the products by 2−4 kcal/mol (for both basis sets).

The radical spin densities of the transition structures and products display the expected odd−alternate character, although the data at the MP2 level clearly overemphasize the differentiation between positive and negative spin densitites at the different sites (values alternating between +0.6 and −0.6 throughout the ring). In the TSs 0.6−0.7 of the unpaired electron still resides at the approaching OH group (B3LYP/6-311G(2df,p) data), whereas in the products all the unpaired spin is on the carbon centers in ortho and para positions to the addition site, ca. 0.35−0.40 on each. None of the spin remains on the entering OH group.

In Table 1 we list the isotropic radical hyperfine coupling constants (HFCC) of the four different products computed at the B3LYP6-311G(2df,p)//B3LYP/6-31G(d,p) level. As a result of the high degree of spin contamination in the MP2 calculations, leading to the unphysically high spin components, the MP2 computed HFCCs are 3−4 times those obtained at the B3LYP level, and thus not considered further. The presently employed combination of method + basis has previously been used with high accuracy for similar biological radicals,[7,10,15,16,30] and we have reason to believe that they are accurate to within 5−10% deviation from experiment.

As seen from the table, there is a clear distinction in HFCC pattern for the ispo/para vs the ortho/meta adducts. This is caused by the out-of-plane ring proton in the ortho and meta form, giving a HFCC pattern of 40, 3.5, −8, and −12 G for the four ring protons. The large positive coupling on the out-of-plane proton is caused by hyperconjugative interaction between the π cloud of the ring carrying the unpaired spin and the s orbital of the proton in question. For the ipso and para adducts, on the other hand, the OH group is added to a carbon not carrying an addition proton (para: since we are considering models for tyrosine), and hence the four ring protons take the splitting pattern 2 × −9 G and 2 × 3.5 G. Apart from this distinction, it is uncertain if the experimental accuracy is such that it will be possible to distinguish further between the ortho and meta or the ipso and para pairs of products unless isotopically labeled samples are employed. However, using ^{17}O labeled samples, together with ENDOR spectroscopy measurements, in which the signs of the HFCCs can be determined, combined with analysis of the normal proton ESR data as outlined above, a distinction between the four products should be possible.

TABLE 2: ZPE Corrected Relative Energies (kcal/mol) for the Water Elimination Reactions Obtained at Different Levels of Theory as Indicated

system	B3LYP//B3LYP	B3LYP//HF	PMP2//HF	PMP2//MP2
Direct H Abstraction				
phenol + OH	0.0	0.0	0.0	0.0
AC	(not found)	−5.3	−5.0	−7.6
phenoxyl + H_2O	−38.5	−38.1	−36.6	−35.6
Direct Elimination from ortho Adduct				
o-OH adduct	0.0	0.0	0.0	0.0
TS	+11.3	(not found)	(not found)	(+19.1)
phenoxyl + H_2O	−17.7	−18.6	−16.3	−14.4
Water Assisted Elimination from ortho Adduct				
o-OH adduct + H_2O, AC	0.0	0.0	0.0	
TS	+10.4	(+18.7)	(+20.9)	
phenoxyl + $2H_2O$	−15.8	−18.0	−14.5	

B. Direct Hydrogen Abstraction. The reaction energies for the direct H-abstraction by OH will be governed by the difference in O−H bond strength in water (119 kcal/mol) compared with tyrosine/phenol (87 kcal/mol).[31] There is hence a substantial exothermicity involved, ca. 32 kcal/mol, which will serve as a driving force for the abstraction reaction. In previous work on related systems, it has been noted that the DFT levels of theory ocassionally are unable to find a transition barrier for this type of elimination reaction, whereas at the spin projected PMP2 level barriers of 2−5 kcal/mol are noted.[11,12]

Also the current B3LYP/6-31G(d,p) calculations are unable to find a transition state for the direct abstraction reaction: in fact we were unable to even find a stable reactant complex for this system. Instead the reaction proceeds instantaneously once the hydroxyl radical is in the vicinity of the phenolic hydrogen, with the products lying 38.5 kcal/mol below the isolated reactants (ZPE corrected B3LYP/6-311G(2df,p) data, Table 2).The direct hydrogen abstraction was also investigated at the HF and MP2 levels of theory. In both these cases, stable addition complexes could be detected, but no transition structures of relevance could be determined. The TS obtained from a number of trial starting structures, including QST2 and QST3 calculations,[32] eigenmode following routines, etc., instead involved abstraction by OH of the C3−H ring proton, followed by water hydrogen bonding to the phenolic hydrogen. This TS geometry, which most likely is caused by the significant spin contamination, was considered unphysical and hence discarded.

The addition complexes lie 5.0−5.2 kcal/mol below the free reactants at the ZPE corrected B3LYP//HF and PMP2//HF levels and at −7.7 kcal/mol at the corresponding PMP2//MP2 level. The product phenoxyl radical, finally, lies 38.2 (B3LYP//HF), 36.6 (PMP2//HF), and 35.6 (PMP2//MP2) kcal/mol below the free reactants. The (ZPE corrected) effect of the additional hydrogen bond between water and the phenolic oxygen is 6−7 kcal/mol, giving a slightly too endothermic description of the difference in O−H bond strength. The largest discrepancy (2−3 kcal/mol) is observed at the PMP2//MP2 and PMP2//HF levels, whereas the B3LYP//B3LYP and B3LYP//HF data are essentially identical to experiment. All methods employed hence show a consistent picture in terms of the overall exothermicity of the reaction and agree well with observed thermodynamic data. In Figure 4 we display the key geometric parameters for the addition complex and product, respectively.

Again, the apparent lack of (or very small) barriers for reaction supports the very high reaction rate reported by Solar

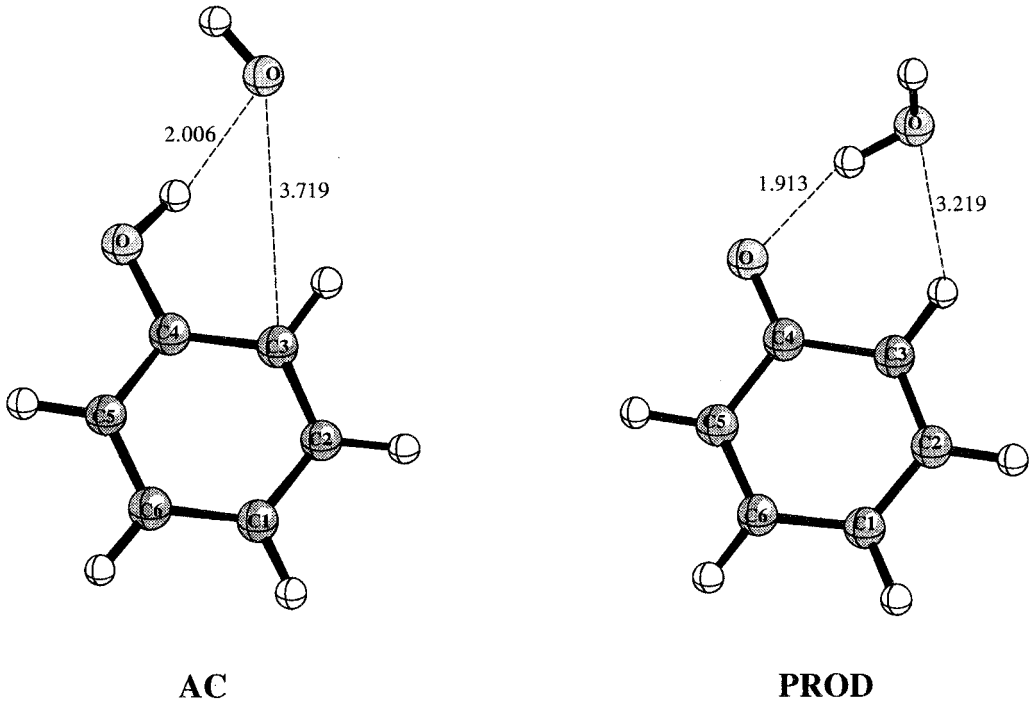

Figure 4. Geometric structures for direct hydrogen atom abstraction by hydroxyl radical, obtained at the MP2/6-31G(d,p) level of theory.

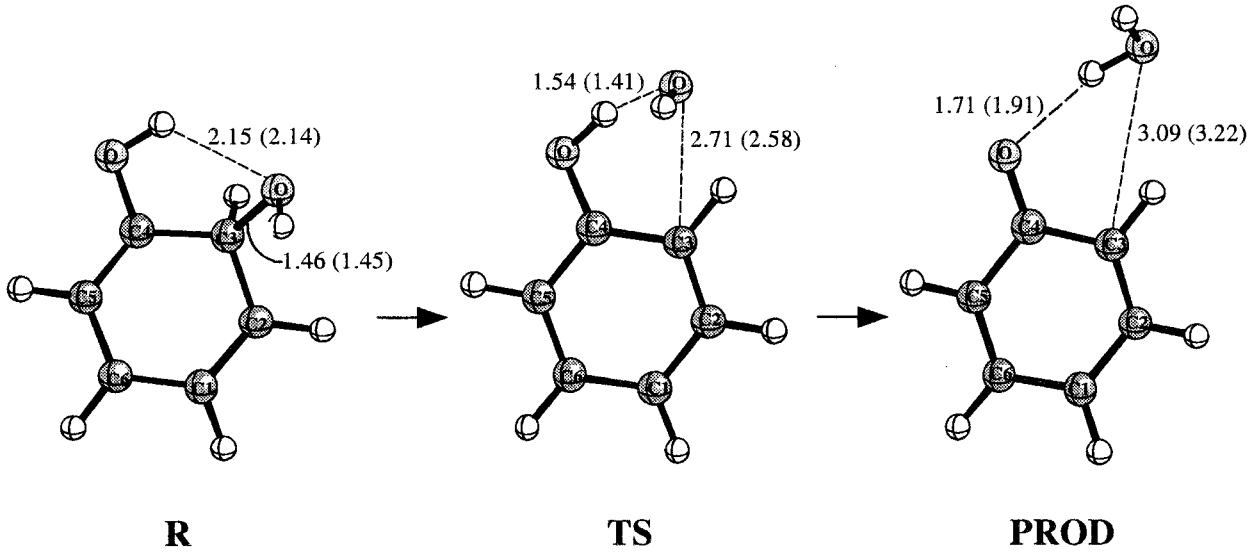

Figure 5. Optimized structures for water elimination from the ortho position, obtained at the B3LYP/6-31G(d,p) and (MP2/6-31G(d,p)) levels.

et al., 6×10^8 dm^3 mol^{-1} s^{-1}.[8] The fact that this rate is estimated to be ca. 1 order of magnitude smaller than the formation of the ortho adduct may be explained in terms of the very restricted accessible surface for direct abstraction: only when the OH group approaches the tyrosine "head-on" will it react by abstraction, wheras at all other angles we may suspect it to instead form an adduct. One should also again bear in mind that for both the ortho and meta positions two different addition sites are available.

C. Water Elimination from Ortho Adduct. In the study by Solar et al., water elimination of the 1,2-dihydroxycyclohexadienyl radical (the ortho OH adduct radical) was also discussed and claimed to occur with a rate constant of 1.8×10^4 s^{-1}, i.e., considerably slower than the previously discussed reaction rates. From simple transition state theory, the 5 orders of magnitude slower reaction rate should correspond to a 6−8 kcal/mol higher transition barrier to elimination. Since the experimental measurements, and also the biologically relevant reactions we wish to model, all occur in aqueous solution, it is possible to imagine that the elimination may take place either directly (with no involvement of additional water molecules) or that it is mediated by hydrogen atom transfer via an additional water, hydrogen bonded to both the phenolic OH and the added/leaving hydroxy group. Both of these systems were investigated, using the B3LYP, HF, and MP2 levels of theory as described above. The resulting optimized structures are displayed in Figures 4 and 5, and in Table 2 we list the energetics of the elimination.

The direct elimination reaction (no additional water) is found to have a very late transition state at both B3LYP and MP2 levels of theory, in which the *o*-hydroxy group has essentially left the ring system (O−C3 distance 2.5−2.7 Å). It is still in a nonplanar arrangement, although closer to the ring plane, than in the reactant. The oxygen of the leaving group hydrogen bonds to the phenolic hydrogen with a distance of 1.41 (MP2)−1.54 (B3LYP) Å. The strained transition state ring system leads to a

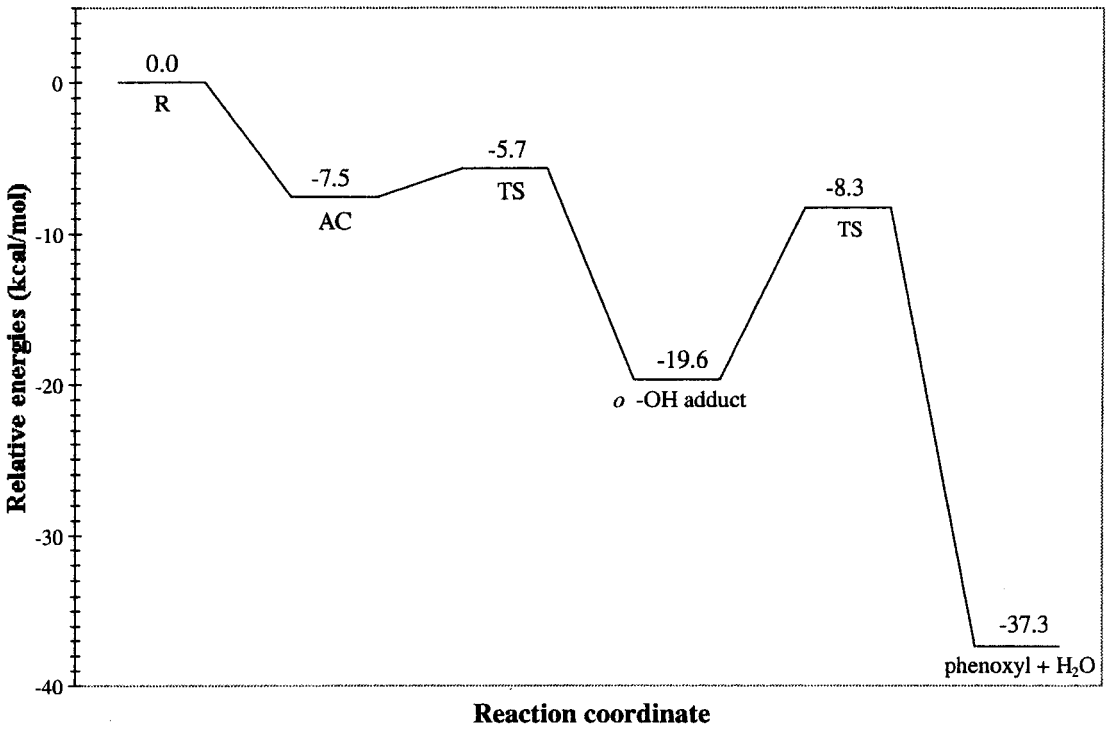

Figure 6. ZPE corrected B3LYP/6-311G(2df,p)//B3LYP/6-31G(d,p) energy surface for OH addition to the ortho position of phenol, and subsequent water elimination.

relatively high barrier to elimination, 11.3 kcal/mol above the reactant at the B3LYP//B3LYP level, and 19.1 kcal/mol at the PMP2//MP2 level. The barrier is hence considerably higher than the 2−5 kcal/mol found for the initial addition reactions. This is in accordance with the slower reaction rate, although the difference in barrier heights appears to be too large at the PMP2 level. Recall, however, that the ortho adduct reactant already lies ca. 20 kcal/mol below the initial starting compounds. The resulting product, which is identical to that from the direct hydrogen abstraction, lies 14.4−18.6 kcal/mol below the reactant, thus yielding a highly exothermic overall reaction.

If we allow the system to use an external water molecule for the elimination, we can form a doubly hydrogen bonded addition complex. The external water is aligned such that it can extract the phenolic hydrogen and simultaneously donate one of its hydrogens to the leaving *o*-hydroxy group, see Figure 5. The optimized addition complexes differ somewhat between HF and B3LYP in that HF places the water molecule 0.2 Å further from the atoms it hydrogen bonds to, and closer to the ring plane. Also, the TS geometries differ. The B3LYP structure places the leaving OH group 2.18 Å out from C5, whereas at the HF level the leaving group is instead shifted sideways and interacts most strongly with C4 (distance O−C4 = 1.89 Å; O−C3 = 2.61 Å). In the product structures, both of the water molecules are oriented such that the hydrogen bonded sequence lies in the ring plane and the additional protons are rotated perpendicular to the plane. The HF hydrogen bonded distances are also here ca. 0.2 Å longer than those from the B3LYP optimization.

At the B3LYP//B3LYP level, the inclusion of the additional water leads to a slight reduction of the barrier (ca. 1 kcal/mol) and a 1.5 kcal/mol less exothermic reaction. The PMP2//MP2 barrier for the direct elimination (19.1 kcal/mol) is similar to those at the B3LYP//HF and PMP2//HF water-assisted eliminations (18.7, 20.9 kcal/mol, respectively). It thus seems that the additional solvent molecule will not have any considerable impact on the elimination reaction.

Conclusions

In the present paper, we have investigated the full potential energy surfaces for hydroxy radical addition to phenol and different elimination reactions yielding the phenoxyl radical, as a model system for the generation of tyrosyl radicals observed in biological media. It is concluded that the ipso and ortho ring adducts on one hand, and the meta and para products on the other, share common reactant complexes, lying 2−9 kcal/mol below the isolated reactants. The energetically favored AC is that leading to the ipso or ortho product.

The barriers to addition are between 1 and 6 kcal/mol at the PMP2//HF and B3LYP//B3LYP levels, with the lowest barriers for ortho and para addition and the highest barrier for the ispo conformer. Taking into account the fact that there are two ortho positions available but only one para and that the para position is sterically crowded in the full amino acid tyrosine, the relative barrier heights for the different addition sites agree well with the observed product yields in phenol[10] vs tyrosine.[8] Spin projection of the HF and MP2 data was proven essential for the transition barriers, whereas the HF surface led to negative barriers when performing single-point B3LYP calculations. The reason for this can be sought in both the addition complexes and the TS geometries. The HF optimized ACs place the incoming OH group further out than does B3LYP, which hence raises the B3LYP//HF addition complex energies. On the other hand, the HF optimized transition structures are later along the reaction coordinate (shorter ring-OH distances) than the B3LYP geometries, and we will hence already be on the downhill path to the product when performing the B3LYP//HF calculations.

The relative product stabilities, finally, predict the ortho adduct to the be most stable one, followed by ipso, para, and (least stable) meta. Again, the data supports the ortho product to be of highest yield, although the remaining products fall in the wrong order (cf. Figure 1). It thus seems that the factors

governing the addition reactions are a combination of kinetics (barrier heights) and thermodynamics (product stabilities).

The generation of tyrosyl (phenoxyl) radicals has been shown to proceed either via a direct abstraction of the phenolic hydrogen by a hydroxyl radical or through water elimination of the *o*-hydroxy phenyl radical. The direct elimination reaction turned out to be very difficult to study. At the B3LYP/6-31G-(d,p) level, no addition complex or transition state could be found: instead the OH radical immediatly takes the phenolic hydrogen to form water in a barrierless reaction. At the HF and MP2 levels, on the other hand, the TS involves removal of one of the ring protons and was considered unphysical. Most likely there will be a small barrier to elimination, as observed for similar reactions involving the histidine model imidazole.[10] Also in those studies did the B3LYP method have difficulties locating a stable addition complex and transition barrier. The overall reaction energy is exothermic by ca. 39 kcal/mol, which agrees well with the experimental difference in O−H bond strengths.

For the water elimination from the ortho adduct, both the direct and the water-assisted pathways displayed a transition barrier of between 11 (B3LYP) and 19 (PMP2) kcal/mol, which explains the ca. 5 orders of magnitude slower rates reported for this reaction compared with those for the OH addition reactions. Again, the HF optimized transition structures deviate considerably from the B3LYP ones and are less likely to be correct. Also, here the ab initio calculations suffer from severe spin contamination. Interestingly, the water-assisted pathway displays an almost identical energy surface to the direct elimination, indicating that the solvent does not actively parttake in the formation of the tyrosyl radicals. In Figure 6, we show the B3LYP//B3LYP computed reaction profile for OH addition to the ortho position of phenol, and the subsequent water elimination.

Taken together, it is clear that the presently computed energy surfaces agree overall with the experimentally reported reaction rates for addition vs elimination. However, the data cannot fully explain the differences in reaction rates and product mixtures. This also holds if we take into account the statistical distribution of addition sites (ratio 2:1 between ortho or meta vs ipso or para). Assuming the experimental data to be correct, it is thus clear that a more dynamical or Monte Carlo-type approach is required to determine the relative product distributions, possibly also including the effects of temperature and the surrounding medium in a more explicit fashion. Work along these lines is currently in progress.

Acknowledgment. The Swedish Natural Sciences Research Council (NFR) and the KK foundation are gratefully acknowledged for financial support. We also acknowledge the Center for Parallel Computing (PDC) in Stockholm for grants of computer time.

References and Notes

(1) *Encyclopedia of Molecular Biology and Molecular Medicine*; Meyers, R. A., Ed.; VCH: Weinheim, 1996.

(2) Newcomb, T. G.; Loeb, L. A. In *DNA Damage and Repair, Vol. 1: DNA Repair in Prokaryotes and Lower Eukaryotes*; Mickoloff, J. A., Hoekstra, M. F., Eds; Humana Press Inc.: Totowa, NJ, 1998. Von Sonntag, C. *The Chemical Basis of Radiation Biology*; Taylor & Francis: London, 1987.

(3) Dizdaroglu, M.; Gajewski, E.; Reddy, P.; Margolis, S. A. *Biochemistry* **1989**, *28*, 3625. Dizdaroglu, M. In *Ionizing Radiation to DNA: Molecular Aspects*; Wallace, S. S., Painter, R. B., Eds; Wiley-Liss, Inc.: New York, 1990.

(4) Leeuwenburgh, C.; Rasmussen, J. E.; Hsu, F. F.; Mueller, D. M.; Pennathur, S.; Heinecke, J. W. *J. Biol. Chem.* **1997**, *272*, 3520.

(5) cf. Stubbe, J.; van der Donk, W. A. *Chem. Rev.* **1998**, *98*, 705, and references therein.

(6) See, e.g, Hoganson, C. W.; Sahlin, M.; Sjöberg, B.-M.; Babcock, G. T. *J. Am. Chem. Soc.* **1996**, *118*, 4672. Tommos, C.; Tang, X.-S.; Warncke, K.; Hoganson, C. W.; Styring, S.; McCracken, J.; Diner, B. A.; Babcock, G. T. *J. Am. Chem. Soc.* **1995**, *117*, 10325. Un, S.; Atta, M.; Fintecave, M.; Rutherford, A. W. *J. Am. Chem. Soc.* **1995**, *117*, 10713. Warncke, K.; Babcock. G. T.; McCracken, J. *J. Am. Chem. Soc.* **1994**, *116*, 7332.

(7) cf. Himo, F.; Gräslund, A.; Eriksson, L. A. *Biophys. J.* **1997**, *72*, 1556. O'Malley, P. J.; Ellson, D. *Biochim. Biophys. Acta* **1997**, *1320*, 65. Qin, Y.; Wheeler, R. A. *J. Am. Chem. Soc.* **1995**, *117*, 6083. Chipman, D. M.; Liu, R.; Zhou, X.; Pulay, P. *J. Chem. Phys.* **1994**, *100*, 5023. Liu, R.; Zhou, X. *Chem. Phys. Lett.* **1993**, *207*, 185.

(8) Solar, S.; Solar, W.; Getoff, N. *J. Phys. Chem.* **1984**, *88*, 2091.

(9) Feitelson, J.; Hayon, E. *J. Phys. Chem.* **1973**, *77*, 10.

(10) Raghavan, N. V.; Steenken, S. *J. Am. Chem. Soc.* **1980**, *102*, 3495.

(11) Llano, J.; Eriksson, L. A. *J. Phys. Chem. B* **1999**, *103*, 5598.

(12) Wetmore, S. D.; Boyd, R. J.; Llano, J.; Lundqvist, M. J.; Eriksson, L. A. In *Recent Advances in Density Functional Methods, Vol. 3*; Barone, V., Bencini, A., Fantucci, P., Eds.; World Scientific: Singapore, in press.

(13) Wetmore, S. D.; Eriksson, L. A.; Boyd, R. J. *J. Chem. Phys.* **1998**, *109*, 9451, and references therein.

(14) Himo, F.; Eriksson, L. A.; Blomberg, M. R. A.; Siegbahn, P. E. M. *Int. J. Quantum Chem. Biophys. Q.*, in press.

(15) Wise, K. E.; Pate, J. B.; Wheeler, R. A. *J. Phys. Chem. B* **1999**, *103*, 4764.

(16) Himo, F.; Babcock, G. T.; Eriksson, L. A. *Chem. Phys. Lett.* **1999**, *313*, 374.

(17) cf. Hehre W. J.; Radom, L.; Schleyer, P. v. R.; Pople, J. A. *Ab initio Molecular Orbital Theory*; Wiley: New York, 1986.

(18) (a) Becke, A. D. *J. Chem. Phys.* **1993**, *98*, 5648. (b) Lee, C.; Yang, W.; Parr, R. G. *Phys. Rev.* **1988**, *B37*, 785. (c) Devlin, P. J.; Chablowski, C. F.; Frisch, M. J. *J. Phys. Chem.* **1994**, *98*, 11623.

(19) (a) Krishnan, R.; Binkley, J. S.; Pople, J. A. *J. Chem. Phys.* **1980**, *72*, 650. (b) McLean, A. D.; Chandler, G. S. *J. Chem. Phys.* **1980**, *72*, 5639. (c) Frisch, M. J.; Binkley, J. S.; Pople, J. A. *J. Chem. Phys.* **1984**, *80*, 3265.

(20) Sekusak, S.; Güsten, H.; Sabljic, A. *J. Chem. Phys.* **1995**, *102*, 7504.

(21) Melissas, V. S.; Truhlar, D. G. *J. Phys. Chem.* **1994**, *98*, 875.

(22) Gonzalez, C.; McDouall, J. J. W.; Schlegel, H. B. *J. Phys. Chem.* **1990**, *94*, 7467.

(23) McKee, M. L. *J. Phys. Chem.* **1993**, *97*, 10971.

(24) Alvarez-Idaboy, J.; Diaz-Acosta, I.; Viver-Bunge, A. *J. Comput. Chem.* **1998**, *19*, 811.

(25) (a) Martell, J. M.; Mehta, A. K.; Pacey, P. D.; Boyd, R. J. *J. Phys. Chem.* **1995**, *99*, 8661. (b) Martell, J. M.; Boyd, R. J. *J. Phys. Chem.* **1995**, *99*, 13402.

(26) Skokov, S.; Wheeler, R. A. *Chem. Phys. Lett.* **1997**, *271*, 251.

(27) cf. (a) Malkin, V. G.; Malkina, O. L.; Eriksson, L. A.; Salahub, D. R. In *Modern Density Functional Theory: A Tool for Chemistry*; Seminario, J. M., Politzer, P., Eds.; Elsevier: Amsterdam, 1995; pp 273−346. (b) Barone, V. In *Recent Advances in Density Functional Methods, Vol. 1*; Chong, D. P., Ed.; World Scientific: Singapore, 1995; pp 287−334.

(28) *Gaussian 94* (Revision E.2), Frisch, M. J.; Trucks, G. W.; Schlegel, H. B.; Gill, P. M. W.; Johnson, B. G.; Robb, M. A.; Cheeseman, J. R.; Keith, T. A.; Peterson, G. A.; Montgomery, J. A.; Raghavachari, K.; Al-Laham, M. A.; Zakrzewske, V. G.; Ortiz, J. V.; Foresman, J. B.; Cioslowski, J.; Stefanov, B. B.; Nanayakkara, A.; Challacombe, M.; Peng, C. Y.; Ayala, P. Y.; Chen, W.; Wong, M. W.; Andres, J. L.; Replogle, E. S.; Gomperts, R.; Martin, R. L.; Fox, D. J.; Binkley, J. S.; Defrees, D. J.; Baker, J.; Stewart, J. P.; Head-Gordon, M.; Gonzalez, C.; Pople, J. A. Gaussian Inc.: Pittsburgh, PA, 1995.

(29) *Gaussian 98* (Revision A.6) Frisch, M. J.; Trucks, G. W.; Schlegel, H. B.; Scuseria, G. E.; Robb, M. A.; Cheeseman, J. R.; Zakrzewski, V. G.; Montgomery, J. A., Jr.; Stratmann, R. E.; Burant, J. C.; Dapprich, S.; Millam, J. M.; Daniels, A. D.; Kudin, K. N.; Strain, M. C.; Farkas, O.; Tomasi, J.; Barone, V.; Cossi, M.; Cammi, R.; Mennucci, B.; Pomelli, C.; Adamo, C.; Clifford, S.; Ochterski, J.; Petersson, G. A.; Ayala, P. Y.; Cui, Q.; Morokuma, K.; Malick, D. K.; Rabuck, A. D.; Raghavachari, K.; Foresman, J. B.; Cioslowski, J.; Ortiz, J. V.; Stefanov, B. B.; Liu, G.; Liashenko, A.; Piskorz, P.; Komaromi, I.; Gomperts, R.; Martin, R. L.; Fox, D. J.; Keith, T.; Al-Laham, M. A.; Peng, C. Y.; Nanayakkara, A.; Gonzalez, C.; Challacombe, M.; Gill, P. M. W.; Johnson, G.; Chen, W.; Wong, M. W.; Andres, J. L.; Gonzalez, C.; Head-Gordon, M.; Replogle, E. A.; Pople, J. A. Gaussian, Inc.: Pittsburgh, PA, 1998.

(30) Wetmore, S. D.; Himo, F.; Boyd, R. J.; Eriksson, L. A. *J. Phys. Chem. B* **1998**, *102*, 7484. Wetmore, S. D.; Boyd, R. J.; Eriksson, L. A. *J. Phys. Chem. B* **1998**, *102*, 5369. Lassmann, G.; Eriksson, L. A.; Himo, F.; Lendzian, F.; Lubitz, W. *J. Phys. Chem. A* **1999**, *103*, 1283.

(31) McMillen, D. F.; Golden, D. M. *Annu. Rev. Phys. Chem.* **1982**, *33*, 493.

(32) Peng, C.; Schlegel, H. B. *Isr. J. Chem.* **1994**, *33*, 449. Peng, C.; Ayala, P. Y.; Schlegel, H. B.; Frisch, M. J. *J. Comput. Chem.* **1996**, *17*, 49.